l dependence of dielectronic recombination from a continuum of finite bandwidth in a static electric field

E. S. Shuman, C. M. Evans, and T. F. Gallagher
Department of Physics, University of Virginia, Charlottesville, Virginia 22904-4714, USA
(Received 8 August 2003; revised manuscript received 24 December 2003; published 1 June 2004)

It should be possible to separate experimentally the contributions to dielectronic recombination (DR) of energetically unresolved intermediate autoionizing Rydberg *nl* states using electric fields. This notion is based on two essential ideas. First, electric fields enhance the DR rate by Stark-mixing low-*l* states with high autoionization rates with high-*l* states with low autoionization rates. Second, the field at which an *l* state becomes Stark mixed is determined by its quantum defect, a known function of *l*. Consequently, the electric-field dependence of the DR rate should reflect the *l* dependence of the autoionization rates and thus the contributions of the zero-field *nl* states to the DR rate. This notion cannot be tested experimentally by examining true DR. However, it can be tested by studying DR from a continuum of finite bandwidth (CFB), for in this case the intermediate Rydberg *nl* states are restricted to a single value of *l*. Specifically, we have examined the electric-field dependence of DR from two CFB's, the Ba $6p_{3/2}11d$ and $6p_{3/2}8g$ states. In these two cases the intermediate autoionizing Rydberg states are restricted to the Ba $6p_{1/2}nd$ and $6p_{1/2}ng$ states ($l=2$ and 4), which have quantum defects of 0.25 and 0.02, respectively. For the same *n* they are Stark mixed at fields differing by an order of magnitude. We show experimentally that enhancement of the DR rate occurs at fields differing by a factor of 10 for *nd* and *ng* states of the same *n*, as expected, confirming that the field dependence of DR can be used to extract information about the contributions of energetically unresolved *l* states to the zero-field DR rate.

DOI: 10.1103/PhysRevA.69.063402 PACS number(s): 32.60.+i, 34.80.Lx

I. INTRODUCTION

Dielectronic recombination (DR), the process by which an ion and an electron recombine via a doubly excited autoionizing Rydberg state, is the primary recombination process in high-temperature laboratory and astrophysical plasmas [1,2]. While the importance of DR is in plasmas, much of the present understanding of DR has come from controlled DR experiments using other techniques [3–6]. The most fruitful has been the use of storage rings, and DR measurements of unprecedented clarity have been conducted using them [6–9]. However, DR is a collision process, and all impact parameters of the collision, or, equivalently, relative orbital angular momenta of the colliding electron and ion, can occur. This angular momentum becomes the orbital angular momentum of the intermediate autoionizing *nl* state of DR. In some cases a few low-*l* states of the same *n* are energetically resolved, but the high-*l* states are not. Throughout this paper we follow the general convention that *n*, *l*, and *m* are the principal, orbital, and azimuthal angular momentum quantum numbers, respectively, of the Rydberg electron. Recent calculations have suggested that high-*l* states may in fact make more significant contributions to the DR rate than previously thought [9,10]. Although high-*l* states are not energetically resolved in DR, the effects of electric fields on different *l* states are very different because of their *l*-dependent quantum defects, and here we suggest that using the electric-field dependence of DR may provide a useful way of determining the contributions of different *l* states to the DR rate.

In this paper we first outline the essential idea behind the notion of using field effects as a probe of the *l* contributions to DR. We then show the result of a model calculation of DR. Most important, we describe an experiment that verifies that an electric field has a vastly different effect on DR for entrance channels leading to $l=2$ and 4 of the intermediate autoionizing state. While control of *l*, or, equivalently, the impact parameter, is impossible in true DR, it is possible when studying DR from a continuum of finite bandwidth [11], and we take advantage of this important difference.

II. THE EFFECT OF AN ELECTRIC FIELD ON DIELECTRONIC RECOMBINATION

In storage ring DR experiments the *n* but not the *l* of the intermediate Rydberg states can often be resolved. Here we describe how the field effect provides information about the contributions of energetically unresolved *l* states using Ba as an example. DR of Ba^+ with a free electron via the $6p_{1/2}nl$ states can be thought of as a two-step process, capture, followed by radiative stabilization [12],

$$\text{Ba } 6s_{1/2} + e^- \rightarrow \text{Ba } 6p_{1/2}nl \rightarrow \text{Ba } 6s_{1/2}nl + h\nu. \qquad (1)$$

We shall for the moment assume that $m=0$, which implies that the direction of the electron's motion is the quantization axis. Since capture is the inverse of autoionization, the capture rate can be represented by a constant times the autoionization rate by the principle of detailed balance. After capture, the electron in the Ba $6p_{1/2}nl$ state can either radiatively decay to the bound Ba $6s_{1/2}nl$ state or autoionize into the continuum. Thus, $\Gamma(nl)$, the contribution to the DR rate of the $6p_{1/2}nl$ state, can be represented by [12]

$$\Gamma(nl) = \beta A_{\mathrm{AI}}(nl)\frac{A_R}{A_{\mathrm{AI}}(nl) + A_R}. \tag{2}$$

Here β is a constant, $A_{\mathrm{AI}}(nl)$ is the autoionization rate of the nl state, and A_R is the radiative decay rate from $6pnl$ to $6snl$. The rate of the radiative decay process of Eq. (1) is independent of n and l since it is the Ba^+ $6p_{1/2} \rightarrow 6s_{1/2}$ transition with the outer electron remaining a spectator during the process. Inspection of Eq. (2) reveals that, except in cases where $A_{\mathrm{AI}}(nl) \approx A_R$,

$$\Gamma(nl) = \beta A_<, \tag{3}$$

where $A_<$ is the lesser of $A_{\mathrm{AI}}(nl)$ and A_R. To an excellent approximation, $A_{\mathrm{AI}}(nl) = a(l)n^{-3}$, where $a(l)$ is a rapidly decreasing function of l. Typically, the major contribution to the DR rate comes from low-l states for which $A_{\mathrm{AI}}(nl) > A_R$, and the total contributions of the l states of a given n to the DR rate, $\Gamma(n)$, can be easily determined by simply counting the states for which $A_{\mathrm{AI}}(nl) > A_R$.

For hydrogenic states any electric field converts the nl states to nk Stark states which are linear superpositions of nl states and, to a first approximation, have autoionization rates equal to the average autoionization rate of all the l states of the same n and m, where the quantization axis is the field direction [13–15]. If the average autoionization rate exceeds the radiative rate, then all Stark states contribute to DR, which raises the rate [13,14]. In essence, the field transfers the excess autoionization rates of the low-l states to the high-l states. If the radiative decay rate is much higher or lower than the autoionization rates of all the nl states, then the field has no effect on DR.

Of course, DR occurs only in nonhydrogenic atoms, which have finite-sized cores and l-dependent quantum defects, resulting in a distinctly nonhydrogenic Stark effect. To be precise, for any given field only the states of $l \geqslant l_E$ are converted to Stark states while those of $l < l_E$ remain angular momentum states. In other words, the l_E state is the lowest l state converted to a Stark state. We shall shortly provide a more precise definition of l_E. Increasing the field decreases l_E, the boundary for Stark mixing. The onset of field enhancement of the DR rate occurs when l_E decreases to the value at which an l state with an autoionization rate exceeding the radiative rate is Stark mixed with higher-l states, for which the opposite is true. The l dependence of the quantum defect can arise from the electric multipole moments of an ion core of total angular momentum 1 or greater [16] or from the polarizability of any ionic core [17]. We here restrict our attention to the case in which the quantum defects are due to core polarization since the Ba^+ $6p_{1/2}$ ion falls into this category.

To an excellent approximation the binding energy of a nonpenetrating nl state is given by the hydrogenic energy with a small correction due to the quantum defect [17],

$$W_{nl} = \frac{-1}{2n^2} - \frac{\delta_l}{n^3}. \tag{4}$$

We use atomic units unless specified otherwise. For high-l states the quantum defect is due to polarization of the ionic core by the Rydberg atom and is given by [17]

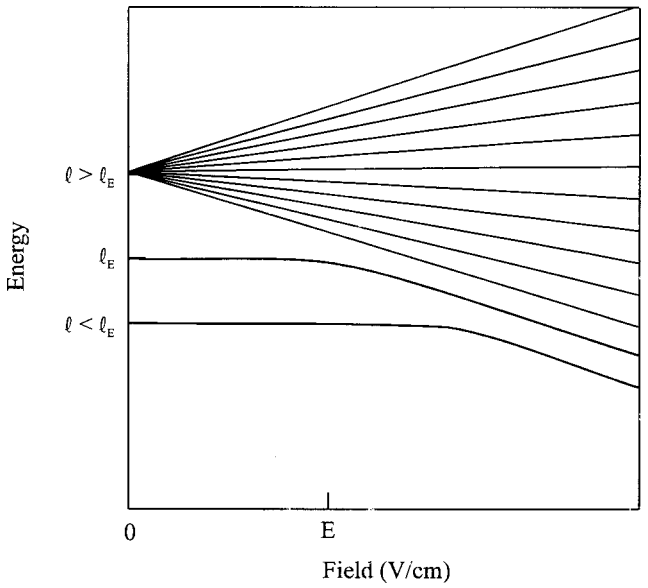

FIG. 1. Electric-field dependence of high-l states. The states of $l > l_E$ are assumed to have negligible quantum defects. The l_E state joins the manifold of Stark states at the field E, while l states of $l < l_E$, which have larger quantum defects, join the Stark manifold at higher fields.

$$\delta_l = n^3 \alpha_d \langle r^{-4} \rangle, \tag{5}$$

where α_d is the polarizability of the ionic core and $\langle r^{-4} \rangle$ is the expectation value of the squared field from the Rydberg electron at the ionic core. To a reasonable approximation [18],

$$\langle r^{-4} \rangle = \frac{1}{n^3(l + 1/2)^5}, \tag{6}$$

so that

$$\delta_l = \frac{\alpha_d}{(l + 1/2)^5}. \tag{7}$$

In the presence of an electric field the high-l states, which have small quantum defects, are converted to Stark states, while the low-l states, which have large quantum defects, are unaffected [19]. Consequently, the field E defines l_E, the lowest-l state converted to a Stark state. States of $l \geqslant l_E$ become what we shall here refer to as Stark states, although they are not the parabolic states. States of $l < l_E$ remain angular momentum states and are unaffected by the field. This notion is depicted graphically in Fig. 1.

If we assume that states of $l > l_E$ have negligible quantum defects, we can relate l_E to E by equating the energy shift δ_{l_E}/n^3 to the Stark shift of the extreme Stark state to define l_E implicitly,

$$\frac{\delta_{l_E}}{n^3} = \frac{3n(n - 1 - l_E)E}{2}. \tag{8}$$

For $l_E \ll n$ this reduces to

$$\delta_{l_E} = \frac{E}{2E_{\mathrm{IT}}}, \tag{9}$$

where E_{IT} is the Inglis-Teller field $1/3n^5$.

If we know the autoionization rates and quantum defects as a function of l it becomes straightforward to calculate the DR rate as a function of the field. In the field m remains a good quantum number, and for small fields n does as well. We can write the recombination rate in the field E through all states of a given value of n and m as

$$\Gamma_E(n,m) = \beta\left[\sum_{l=|m|}^{l=l_E-1} \frac{A_{\mathrm{AI}}(nl)A_R}{A_{\mathrm{AI}}(nl)+A_R} + (n-l_E)\,\frac{\overline{A}_n(E)A_R}{\overline{A}_n(E)+A_R}\right], \tag{10}$$

where $\overline{A}_n(E)$ is the average autoionization rate of the $l \geqslant l_E$ states. The sum in the square brackets of Eq. (10) is the contribution from the low-l states, and the second term is that from the former high-l states, which have become Stark states. Given that we are adding the rates, a reasonable approximation for $\overline{A}_n(E)$ is

$$\overline{A}_n(E) = \frac{\sum_{l=l_E}^{l=n-1} A_{\mathrm{AI}}(nl)}{n-l_E}. \tag{11}$$

If all m states make equal contributions to the DR rate, then summing the contributions for all m states yields the contribution of a given n state to the DR rate vs field. Explicitly,

$$\Gamma_E(n) = \sum_{m=-(n-1)}^{n-1} \Gamma_E(n,m). \tag{12}$$

To illustrate the field dependence graphically, we show in Fig. 2 $\Gamma_E(25,0)$ as a function of field for a model atom. In this figure, the autoionization rates in atomic units for $l=0-4$ are $0.09n^{-3}$, $0.02n^{-3}$, $0.05n^{-3}$, $0.31n^{-3}$, and $0.05n^{-3}$, respectively [20]. The autoionization rates for $l \gg 4$ are given by $A_{nl}=24e^{-1.5l}n^{-3}$, which approximates those of the Ba $6p_{1/2}nl$ states [21]. We assume that the quantum defects of $l \geqslant 4$ states are determined from Eq. (7) using a core polarizability of $120a_0^3$, and that the quantum defects of the $l=0-3$ states are given by 0.5, 0.3, 0.2, and 0.1, respectively. We have used two values for the radiative decay rate, $A_R=3.88\times10^{-10}$ and 3.88×10^{-8}. The former is 10% of the Ba^+ $6p$-$6s$ transition rate, while the latter is ten times it. In both cases there is no field dependence of the DR rate at low field, since only the highest-l states, which have autoionization rates less than the radiative rate, are affected. The DR rate begins to increase at the field at which the l state with an autoionization rate in excess of the radiative rate joins the Stark manifold. For $A_R=3.88\times10^{-10}$ the increase in the DR rate begins at $l=10$ and $E=0.4$ V/cm, and for $A_R=3.88\times10^{-8}$ it begins at $l=7$ and $E=1.5$ V/cm. There is no field dependence at fields at or above the Inglis-Teller field since the Stark mixing is complete. In an experiment, the observed DR rate is a sum over all m states, with a weighting dependent on the experimental geometry. However, even if we assume an equal weighting of m states, and compute $\Gamma_E(25)$ as a function of field for $A_R=3.88\times10^{-10}$ and 3.88×10^{-8}, the field enhancements occur at the same places as in Fig. 2, because l_E does not depend on m.

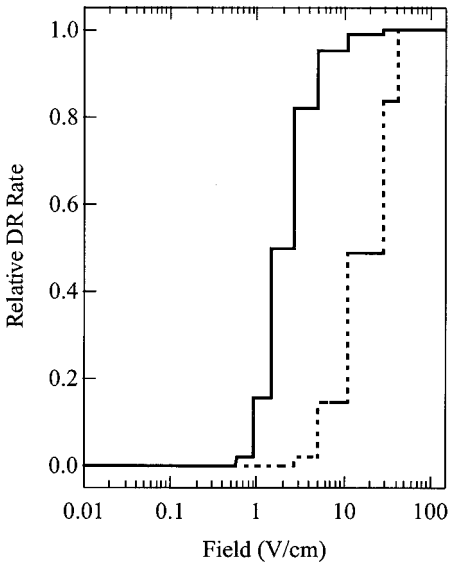

FIG. 2. Relative calculated DR rate $\Gamma_E(nm)$ from Eq. (10) with $n=25$ and $m=0$ plotted as a function of electric field. The proportionality constant β is assumed to be 1. The solid line is for a radiative rate $A_R=3.88\times10^{-10}$ while the dotted line is for $A_R=3.88\times10^{-8}$. (The radiative rate for the Ba^+ $6p\rightarrow6s$ transition is 3.88×10^{-9}.) In both cases the rate at $E=100$ V/cm is normalized to unity.

Figure 2 demonstrates the essential point, that the E-field dependence of the DR rate should reflect the l dependence of the quantum defects and autoionization rates. Consequently, this technique should be useful in analyzing the contributions to DR of energetically unresolved l states in storage ring experiments.

III. DIELECTRONIC RECOMBINATION FROM A CONTINUUM OF FINITE BANDWIDTH

In true DR there is no control of the impact parameter of the electron-ion collisions leading to DR, and hence no control over the l of the Rydberg electron in the intermediate autoionizing state. Consequently, it would be impossible to verify experimentally the notions outlined above by studying true DR. Instead, we have replaced the true continuum with a continuum of finite bandwidth (CFB) [11], allowing us to select the l of the Rydberg electron in the intermediate autoionizing state by choosing different continua of finite bandwidth. In this experiment, either of the two broad autoionizing Ba^+ $6p_{3/2}11d$ or Ba^+ $6p_{3/2}8g$ states converging to the Ba^+ $6p_{3/2}$ limit serves as the continuum of finite bandwidth. Specifically, we have studied the two processes

$$\mathrm{Ba}\ 6p_{3/2}11d \rightarrow \mathrm{Ba}\ 6p_{1/2}nd \rightarrow \mathrm{Ba}\ 6snd + h\nu \tag{13a}$$

and

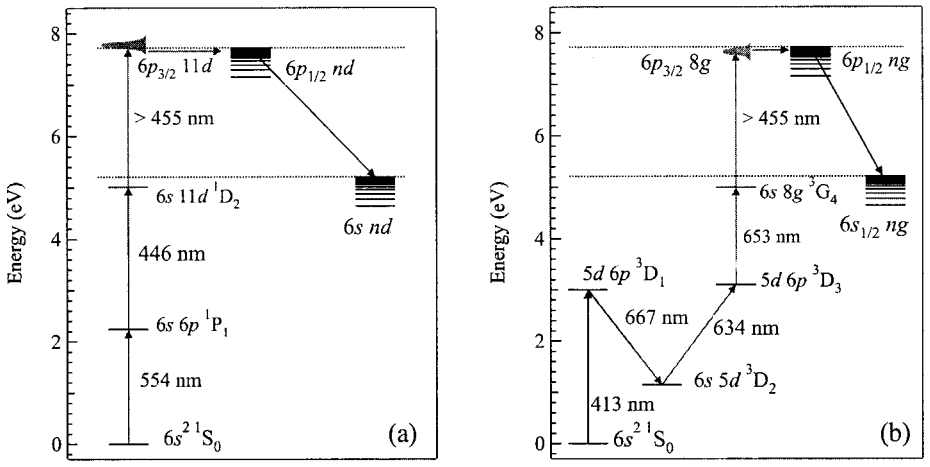

FIG. 3. Barium energy level diagram for dielectronic recombination from a continuum of finite bandwidth. (a) Three dye lasers are used to drive the transitions from the Ba $6s^2$ ground state to the $6p_{3/2}11d$ state, which is the continuum of finite bandwidth. From it, the $11d$ electron can either autoionize into the true continuum or be captured into the degenerate $6p_{1/2}nd$ state (represented by the horizontal arrow). If capture occurs, the $6p_{1/2}nd$ state can either autoionize or decay radiatively to a stable $6snd$ state (represented by the solid arrow). In the latter case, dielectronic recombination has occurred and is detected by field ionization of the $6snl$ Rydberg states. (b) Five dye lasers are used to drive the transitions from the Ba $6s^2$ ground state to the $6p_{3/2}8g$ state, which is the continuum of finite bandwidth. From it, the $8g$ electron can either autoionize into the true continuum or be captured into the degenerate $6p_{1/2}ng$ state (represented by the horizontal arrow). If capture occurs, the $6p_{1/2}ng$ state can either autoionize or decay radiatively down to a stable $6s$ ng state (represented by the solid arrow). In the latter case, dielectronic recombination has occurred and is detected by field ionization of the $6sng$ Rydberg state.

$$\text{Ba } 6p_{3/2}8g \rightarrow \text{Ba } 6p_{1/2}ng \rightarrow \text{Ba } 6sng + h\nu. \quad (13b)$$

The internal transition from the $6p_{3/2}11d(8g) \rightarrow 6p_{1/2}nd(ng)$ state is analogous to capture in true DR. This transition is a quadrupole transition, whereas in true DR it is a dipole transition, an insignificant difference for electron scattering. The $11d(8g)$ state is like a storage ring, and each $11d(8g)$ electron collides with the Ba $6p_{3/2}$ core roughly 20 times before autoionization occurs. The most important difference between true DR and DR from a CFB is the one noted above. In true DR the electron-ion collisions have all possible impact parameters, and the autoionizing Rydberg states resulting from capture of the electron can be in all nl states. In contrast, in DR from a CFB there is only one l value for the entrance channel. The fact that there is only one entrance channel is crucial for this experiment, for it allows us to test our earlier claim that l states with different quantum defects join the Stark manifold, and therefore begin to contribute to the enhancement of DR, at different fields. In this particular experiment we are taking advantage of the difference between true DR and DR from a CFB, i.e., the fact that we can control which low-l state is the entrance channel. It is, however, worth bearing in mind the essential similarity of true DR and DR from a CFB for the study of field effects. In true DR the low-l states have the largest capture rates, so, irrespective of which low-l state we choose as the entrance channel using the CFB, the result is qualitatively the same as for true DR.

For our present purposes the most important difference between the $6p_{1/2}nd$ and $6p_{1/2}ng$ states is the difference in their quantum defects. Specifically, $\delta_d = 0.25$ and $\delta_g = 0.02$, so for a given n the electric fields at which these states become Stark states should be different by an order of magnitude, as discussed in the previous section. If the notions presented in the previous section are correct, for a given value of n the onset of field enhancement of DR should occur at fields differing by the same factor.

IV. EXPERIMENTAL APPROACH

Ba atoms are excited sequentially to the continua of finite bandwidth, either the $6p_{3/2}11d$ state or the Ba $6p_{3/2}8g$ state, using the isolated core excitation approach. The $6p_{3/2}11d$ state is created using three 5 ns Littman dye lasers as shown in Fig. 3(a). The first two lasers are fixed in frequency to drive the transitions

$$6s^2\ ^1S_0 \rightarrow 6s6p\ ^1P_1 \rightarrow 6s11d\ ^1D_2. \quad (14)$$

The third laser drives the transition from the $6s11d$ to the $6p_{3/2}11d$ state, and its frequency is scanned near the Ba^+ $6p_{1/2}$ limit. All three laser pulses overlap in time and space. In essentially the same manner, the $6p_{3/2}8g$ state is created using five 5 ns Littman dye lasers as shown in Fig. 3(b). The first four lasers are fixed in frequency to drive the transitions

$$6s^2\ ^1S_0 \rightarrow 5d6p\ ^3D_1 \rightarrow 6s5d\ ^3D_2 \rightarrow 5d6p\ ^3D_3 \rightarrow 6s8g\ ^3G_4, \quad (15)$$

and these four laser pulses also overlap in time and space. Approximately 20 ns later, the final laser drives the $6s8g\ ^3G_4 \rightarrow 6p_{3/2}8g$ transition. The final laser is delayed to avoid exciting unwanted transitions from short-lived states with the fifth laser. The final laser is scanned in frequency near the Ba^+ $6p_{1/2}$ limit. In both excitations, the dye lasers are pumped by the second and third harmonics of a

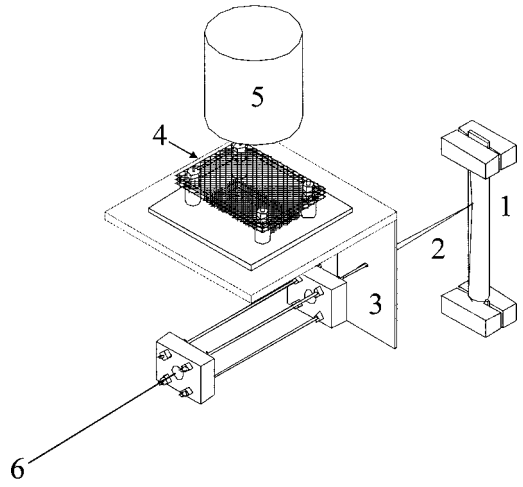

FIG. 4. Schematic diagram of the experimental apparatus showing (1) the oven, (2) the atomic beam, (3) the collimator, (4) the mesh, (5) the microchannel plate detector, and (6) the collinear dye laser beams.

Q-switched Nd:YAG (yttrium aluminum garnet) laser running at a 20 Hz repetition rate.

Aside from the differing excitation schemes, the experiments from the two continua of finite bandwidth are conducted in the same way. As shown in Fig. 4 a thermal beam of barium atoms effuses from a resistively heated oven and passes down the axis of a set of four rods 0.24 cm in diameter and 1.9 cm apart. The lasers counterpropagate to the atomic beam and overlap the beam along the axis of the rods. A fixed voltage can be placed on the rods to create a static field during the excitation. Typically, the polarization of the lasers is parallel to the field so as to excite the $m=0$ states, although similar data are obtained with other polarizations, suggesting that our observations are representative of all $|m| \leqslant 3$ states. Approximately 1 μs after the last laser, a voltage pulse of 1 kV is applied to the rods, producing a 380 V/cm field pulse to ionize any high-lying bound Rydberg states created through DR, and we detect the electrons from these atoms with a microchannel plate detector. This ionization signal is then captured with a gated integrator and recorded as the frequency of the final laser is scanned. The ionization signal can also be recorded as the electric field is swept from 0 to 50 V/cm while the final laser is fixed in frequency. We estimate the stray fields to be 300 mV/cm. As we shall see, this field produces Stark mixing of the *ng* states for states of $n>60$, i.e., within 30 cm^{-1} of the $6p_{1/2}$ ionization limit. For this reason we have focused our attention on states of $n<50$.

V. OBSERVATIONS

In Fig. 5 we show typical scans of the final laser wavelength when observing DR with and without a static field present. The traces presented in Fig. 5 have been normalized to the autoionization signals from their respective continua to remove the differences in the DR signals due to the different energy variations in the number of atoms excited to the two

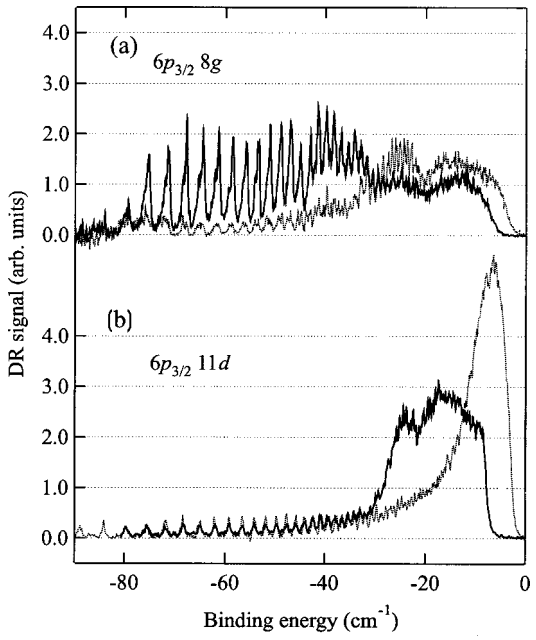

FIG. 5. DR signals obtained by scanning the frequency of the last laser so as to excite the continua of finite bandwidth (a) $6p_{3/2}8g$ and (b) $6p_{3/2}11d$ in the vicinity of the Ba^+ limit. The horizontal energy scale is relative to the $6p_{1/2}$ limit. Shown are signals obtained with zero field (···) and a 1.6 V/cm field (—).

continua of finite bandwidths. In Fig. 5(a) we show the DR signals obtained from the 8*g* CFB with no static field and in the presence of a 1.5 V/cm static field, and in Fig. 5(b) we show DR under the same conditions from the 11*d* CFB. In Fig. 5 we see that in the 1.5 V/cm traces there is a substantial increase in DR from both CFB's as compared to the zero-field traces; however, it is obvious that enhancement is strikingly different depending on whether DR occurs from the 8*g* or 11*d* CFB, i.e., through $l=4$ or 2 intermediate $6p_{1/2}nl$ states. In the 1.5 V/cm traces the enhancement of DR extends to a far lower binding energy for the 8*g* CFB than for the 11*d* CFB. This observation is what we expected to see. What we did not expect to see is that the enhancement of DR from the 8*g* CFB seems to disappear at the energy at which the enhancement of DR from the 11*d* CFB begins to appear.

From Fig. 5 it is apparent that DR via the $6p_{1/2}ng$ states is enhanced at lower field than via the $6p_{1/2}nd$ states of the same *n*. To make accurate measurements of the fields at which the enhancements occur, we have fixed the frequency of the final laser on the zero-field $6p_{1/2}nl$ state and scanned the field in which DR occurs. In Fig. 6 we have plotted the fields at which 50% of the enhancement of the DR rate occurs, vs $1/n^{-5}$ for both the *nd* and *ng* states. The enhancement fields for the *nd* and *ng* states are given by $0.34(1)n^{-5}$ and $0.033(1)n^{-5}$, respectively. In other words, we observe the expected n^{-5} behavior and an order of magnitude difference between the fields for the *d* and *g* states, but our observed values do not agree with the values predicted from Eq. (9), which are $0.16n^{-5}$ and $0.013\ n^{-5}$. In both cases the enhancement fields are a factor of 2 higher than predicted by Eq. (9), and the discrepancy is due to simplifying assumptions used

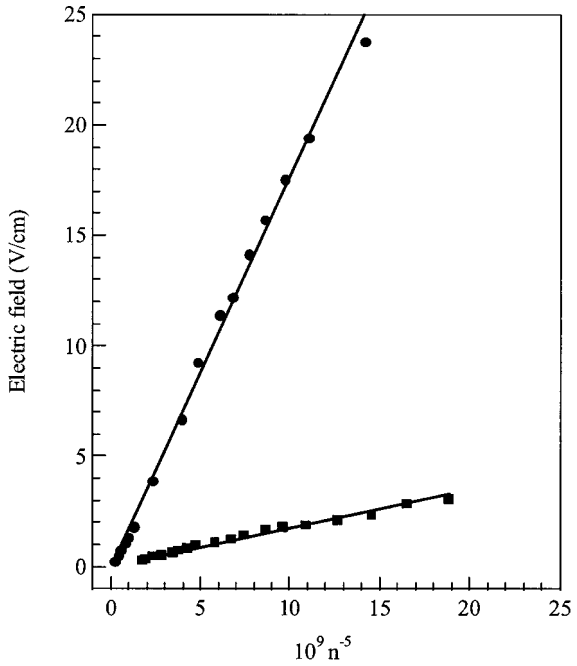

FIG. 6. The electric field at which 50% of the maximum enhancement occurs versus $1/n^5$. (●) *nd* states, (■) *ng* states. The lines represent least-squares fits to $E=b/n^5$ (in atomic units) with (—) $b=0.388\pm0.007$ and (----) $b=0.033\pm0.003$.

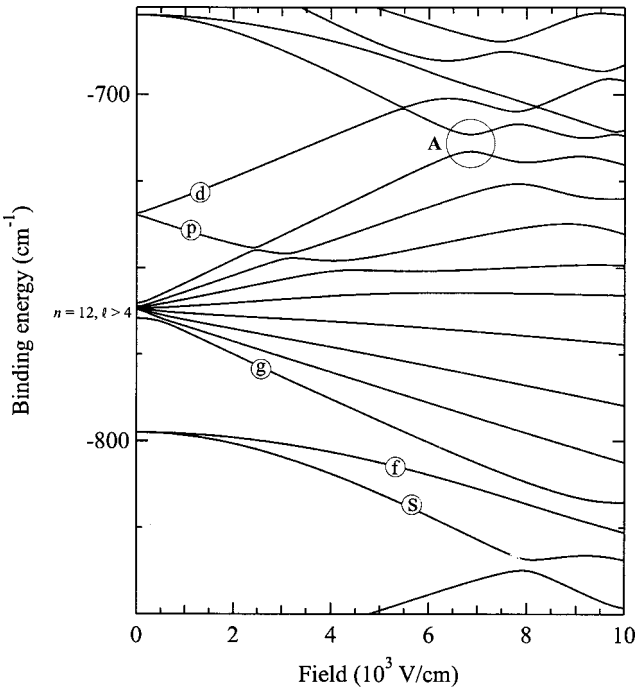

FIG. 7. Energy level diagram of $|m|=0$ states with a Ba $6p_{1/2}$ core in the vicinity of the $n=12$ manifold as a function of the electric field. States adiabatically converted to the zero-field *nl* states are marked as a guide to the reader. Circle A marks the Inglis-Teller field (6888 V/cm) and is also the field at which the *d* state joins the Stark manifold.

in deriving Eq. (9). Let us consider the *nd* states first. The enhancement occurs not at $E=0.16n^{-5}$ but at the Inglis-Teller field. Why this occurs is easily understood by examining the field–energy-level diagram for the Ba $6p_{1/2}nl$ states shown in Fig. 7. As shown, the *nd* state does not have a field-independent energy until it intersects the Stark manifold but is strongly repelled by the $(n+1)p$ state and only intersects the Stark manifold at the Inglis-Teller field. The observed enhancement field for the *ng* states is also a factor of 2 higher than that predicted by Eq. (9), for a similar reason; it has a nonzero Stark shift for fields less than that given by Eq. (9). Although Fig. 6 does not agree perfectly with our simple model, it dramatically illustrates our main point, that the field dependence of the DR enhancement is different depending on the *l* state through which DR occurs.

An important effect noted above is the fact that the enhancement of the DR rate in *ng* states decreases dramatically at the field at which the enhancement of the *nd* states occurs, i.e., at the Inglis-Teller field. Once the field has increased to the field at which the *ng* state is mixed into the manifold, further increases in the field do not increase the capture rate but do increase the loss due to rapid autoionization through the acquired $l<4$ character, which lowers the DR rate as the field approaches the Inglis-Teller field. DR from the $6p_{3/2}11d$ CFB is somewhat simpler than from the $6p_{3/2}8g$ CFB, because the Ba $6p_{1/2}nd$ states do not join the Stark manifold until the Inglis-Teller field, as is shown by Fig. 6. Since the *nd* state does not mix into the manifold until the Inglis-Teller limit, no other *l* states can be added to the manifold at a higher field, and the decline in the DR rate noted in the *g* states cannot occur. Stated another way, because the *nd* states join the Stark manifold at the Inglis-Teller field, there are only two cases, no Stark mixing and full Stark mixing, as has been shown previously [22,23].

While our focus has been on the electric fields at which the enhancement occurs, quantitative measurements of the enhancements are also useful. By making a series of wavelength scans such as those shown in Fig. 5 we have determined the enhancement factors $\mathcal{R}_{nl}(E)$ for different *nl* states as a function of the field. Explicitly, we define the enhancement factor as the ratio of the DR signal in the field to the zero-field signal. In Fig. 8(a) we show the enhancement factors for *ng* states of $39\leqslant n\leqslant 48$, and in Fig. 8(b) we show the corresponding enhancement factors for the *nd* states.

As shown by Fig. 8 the maximum enhancement factors for the *ng* and *nd* states are $\mathcal{R}_{ng}(E)=13(3)$ and $\mathcal{R}_{nd}(E)=9(2)$. These values can be compared to estimates for the enhancement factors obtained by following the procedure outlined by Ko *et al.* [22]. Specifically, we can write the enhancement factor for DR via an *ng* state $\mathcal{R}_{ng}(E)$ as the ratio of the DR rate through the *g* character of all the $m=0$ Stark states (for $0.03n^{-5}<E<0.13n^{-5}$) to the DR rate through the zero-field *ng* state. Explicitly,

$$\mathcal{R}_{ng}(E)=\frac{(n-4)\beta\overline{R}_{ng}(E)A_R/[\overline{R}_{ng}(E)+\overline{A}_n(E)+A_R]}{\beta R(ng)A_R/[R(ng)+A_{\mathrm{AI}}(ng)+A_R]}. \tag{16}$$

Here $\beta R(ng)$ is the capture rate into the $6p_{1/2}ng$ state from the $6p_{3/2}\,8g$ state (the constant β was defined previously),

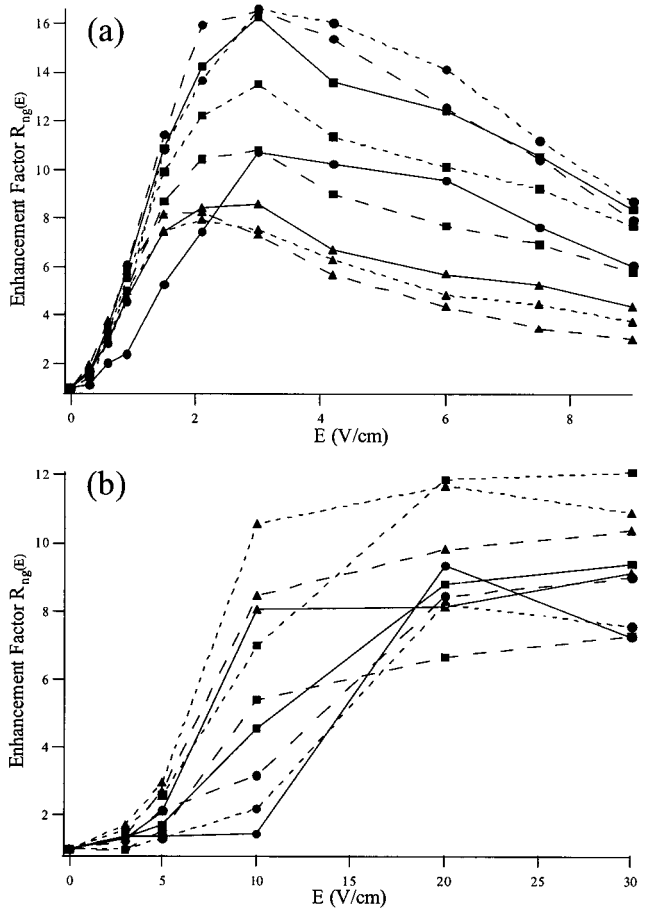

FIG. 8. Enhancement factor $R_{nl}(E)$ vs electric field for the *ng* states (a) and the *nd* states (b) for $39 \leqslant n \leqslant 48$. In both cases the enhancement factor reaches a maximum of roughly 10. In both cases the onset occurs at the fields given in Fig. 6. For the *ng* states (a) the decline at higher fields is due to the admixing of the *nf* states with their rapid autoionization rate. The same symbols are used in (a) and (b), and the data points are joined by straight line segments. 39*l* (●—), 41*l* (●----), 42*l* (●– –), 43*l* (■—), 44*l* (■----), 45*l* (■– –), 46*l* (▲—), 47*l* (▲----), and 48*l* (▲– –),

and $A_{\mathrm{AI}}(ng)$ is its autoionization rate into the 6*s* and 5*d* continua. We use $\beta\overline{\mathcal{R}}_{ng}(E)$ for the capture rate into a $6p_{1/2}nk$ Stark state and $\overline{A}_n(E)n^{-4}$ for its autoionization rate into the 6*s* and 5*d* continua. For $0.03n^{-5} < E < 0.13n^{-5}$ there are $n-4$ Stark states, leading to that factor in the numerator. Since $\overline{R}_{ng}(E) = R(ng)/(n-4)$, Eq. (16) can obviously be simplified. It can be further simplified by using the *n* scalings of the autoionization and capture rates. Explicitly, $R(ng) = r_g n^{-3}$, $A_{\mathrm{AI}}(ng) = a_g n^{-3}$, and $\overline{A}_n(E) = a_n(E)n^{-4}$, and using these scalings Eq. (16) can be written as

$$\mathcal{R}_{ng}(E) = \frac{r_g n^{-3} + a_g n^{-3} + A_R}{r_g n^{-4} + a_n(E) n^{-4} + A_R}. \tag{17}$$

An analogous expression can be written for $\mathcal{R}_{nd}$, the enhancement factor for DR via the $6p_{1/2}nd$ states. Using the known values $r_g = 0.02$, $a_g = 0.03$, and the value $a_n(E) = 0.035$, appropriate for $0.013n^{-5} < E < 0.13n^{-5}$ [20,24], we find that, for $n = 45$, $\mathcal{R}_{ng}(E) = 31$, which is a factor of $2\frac{1}{2}$ larger than our measured value. For DR through the $6p_{1/2}nd$ states we use the values $r_d = 0.03$, $a_d = 0.06$, and $a_n(E) = 0.53$ [20,25], appropriate for fields in excess of the Inglis-Teller field. With these values and $n = 45$ we find $\mathcal{R}_{nd}(E) = 7$, in reasonable agreement with our measured values.

We attribute of the discrepancy between the calculated and measured *ng* enhancement to partial Stark mixing of the *nf* states into the Stark manifold. By the time the *ng* states have joined the Stark manifold, the *nf* states have partially joined it, sharing their large autoionization rates with the Stark states and suppressing the DR rate. If the field is large enough to completely admix the *nf* states to the Stark manifold the value of $a_n(E)$ is not 0.035, but 0.345, and $\mathcal{R}_{ng}(E) = 6$. Mixing only 30% of the *nf* state into the Stark manifold leads to $a_n(E) = 13$ and $\mathcal{R}_{ng}(E) = 13$, in agreement with our observations.

VI. CONCLUSION

We have observed a substantial difference in the behavior of DR from a CFB in a static field depending on the *l* state through which recombination occurs. We have shown that the field at which the DR rate enhancement begins is ten times lower when recombination occurs through the *g* states than it is when recombination occurs through the *d* states. We have developed a simple model that agrees reasonably well with the observed results, as well as a more sophisticated calculation which also reproduces our experimental results. These experiments show that by using *E* fields it should be possible to extract information about the *l* dependence of DR rates, even though the high-*l* states are energetically unresolved.

ACKNOWLEDGMENTS

This work has been supported by the U.S. Department of Energy. It is a pleasure to acknowledge helpful comments from C. H. Greene.

[1] H. S. W. Massey and D. R. Bates, Rep. Prog. Phys. **9**, 62 (1942).
[2] A. Burgess, Astrophys. J. **139**, 776 (1964).
[3] D. S. Belić, G. H. Dunn, T. J. Morgan, D. W. Mueller, and C. Timmer, Phys. Rev. Lett. **50**, 339 (1983).
[4] P. F. Dittner, S. Datz, P. D. Miller, P. L. Pepmiller, and C. M. Fou, Phys. Rev. A **35**, 3668 (1987).
[5] R. Ali, C. P. Bhalla, C. L. Cocke, and M. Stockli, Phys. Rev. Lett. **64**, 633 (1990).
[6] T. Bartsch, A. Müller, W. Spies, J. Linkemann, H. Danared, D.

R. DeWitt, H. Gao, Z. Wong, R. Schuch, A. Wolf, G. H. Dunn, M. S. Pindzola, and D. C. Griffin, Phys. Rev. Lett. **79**, 2233 (1997).

[7] T. Bartsch, S. Schippers, A. Müller, C. Brandau, G. Gwinner, A. A. Saghiri, M. Beutelspacher, M. Grieser, D. Schwalm, A. Wolf, H. Danared, and G. H. Dunn, Phys. Rev. Lett. **82**, 3779 (1999).

[8] S. Bohn, S. Schippers, W. Shi, A. Müller, N. Eklöw, R. Schuch, H. Danared, N. R. Badnell, D. M. Mitnik, and D. C. Griffin, Phys. Rev. A **65**, 052728 (2002).

[9] C. Brandau, T. Bartsch, A. Hoffnecht, H. Knopp, S. Schippers, W. Shi, A. Müller, N. Grun, W. Scheid, T. Seih, F. Bosch, B. Franzke, C. Kozhuharov, P. H. Mokler, F. Nolden, M. Steck, T. Stohlker, and Z. Stachum, Phys. Rev. Lett. **89**, 053201 (2002).

[10] D. M. Mitnik, M. S. Pindzola, and N. R. Badnell, Phys. Rev. A **61**, 022705 (2000).

[11] J. P. Connerade, Proc. R. Soc. London, Ser. A **362**, 361 (1978).

[12] A. L. Merts, R. D. Cowan, and N. H. Magee, Jr., Los Alamos Report No. LA-62200-MS, 1976 (unpublished).

[13] V. L. Jacobs, J. Davis, and P. C. Kepple, Phys. Rev. Lett. **37**, 1390 (1976).

[14] V. L. Jacobs and J. Davis, Phys. Rev. A **19**, 776 (1979).

[15] K. A. Safinya, J. F. Delpech, and T. F. Gallagher, Phys. Rev. A **22**, 1062 (1980).

[16] W. H. Clark and C. H. Greene, Rev. Mod. Phys. **71**, 821 (1999).

[17] B. Edlen, in *Spectroscopy I*, edited by S. Flugge, Handbuch der Physik Vol. 27 (Springer, Berlin, 1964).

[18] H. A. Bethe and E. A. Salpeter, *Quantum Mechanics of One and Two Electron Atoms* (Plenum, New York, 1977).

[19] M. L. Zimmerman, M. G. Littman, M. M. Kash, and D. Kleppner, Phys. Rev. A **20**, 2251 (1979).

[20] R. R. Jones and T. F. Gallagher, Phys. Rev. A **39**, 4583 (1989).

[21] R. R. Jones and T. F. Gallagher, Phys. Rev. A **38**, 2846 (1988).

[22] L. Ko, V. Klimenko, and T. F. Gallagher, Phys. Rev. A **59**, 2126 (1999).

[23] J. G. Story, B. J. Lyons, and T. F. Gallagher, Phys. Rev. A **51**, 2156 (1995).

[24] S. M. Jaffe, R. Kachru, H. B. van Linden van den Heuvell, and T. F. Gallagher, Phys. Rev. A **32**, 1480 (1985).

[25] O. C. Mullins, Y. Zhu, E. Y. Xu, and T. F. Gallagher, Phys. Rev. A **32**, 2234 (1985).